LMI 최적화기법을 적용한 H_∞ 제어 시스템의 전력계통 안정화장치(PSS) 설계

論 文
49D - 4 - 1

H_∞ Control Synthesis for Power System Stabilizer Design using LMI Optimization Method

鄭 大 源*・朱 雲 杓**・金 建 中***
(Dae-Won Chung · Oon-Pyo Zhu · Kern-Joong Kim)

Abstract - This paper presents the application of H_∞ control synthesis using LMI optimization method to power system stabilizer(PSS) design. Since power system is usually operated under circumstance of unmeasurable uncertainties and external disturbances, the improvement of small signal stability becomes one of the most important issue for securing system stability and preventing low frequency oscillation phenomena. The LMI optimized H_∞ PSS provides robust performance and guarantees the internal stability under these operating conditions. The global optimal H_∞ norm is found using LMI convex optimization method which is more systematic than standard two Riccati solution method. The design results are simulated for a case study. We verified that the LMI method shows the best performance characteristic among standard Riccati method and conventional lead/lag method.

Key Words : uncertainties, disturbances, robustness, H_∞ control, LMI approach

1. Introduction

The phenomenon of small signal stability of synchronous machine operation has attracted a great deal of attention in the field of modern power systems. Power system stabilizers (PSS) have been widely used in electric power industries to improve this small signal stability. Through the supplementary control of an excitation system and governor system, PSS can suppress low frequency oscillations of a small magnitude and provide extra damping for synchronous machines under uncertain operating conditions. The design of the conventional lead/lag filtered PSS was first proposed in the 1960s and was based on the classical linear control methodology. Each PSS is tuned around one operating condition for providing adequate performance within a certain range of limitations. It has also been found that dynamic properties of power systems are quite different for various operating conditions. The major disadvantage of conventional PSS is that overall system stability can not be guaranteed effectively in the circumstance of varying operating conditions. A lot of research works have been carried out to overcome the kinds of challenges caused by varying operating conditions including system uncertainties. Most researches are mainly based on the traditional design methodology such as eigenvalues (pole) assignment [1], and modern ones such as self-tuning control technique[2, 3], etc. However, H_∞ optimization synthesis[4] has been developed as a way to handle the uncertainties and has achieved robust performance. Robustness requirements in power system control are directly related to improving the small signal stability such as small magnitude and low frequency oscillation problems. Some research on applying H_∞ control synthesis to design PSS has also been presented in some publications and papers [5-9]. These publications have shown that H_∞ controllers can effectively maintain the stability and performance of the system for a wide range of operating conditions in spite of the presence of uncertainties and external disturbances in the system. Some of the publications reported the importance and difficulties in the selection of the weighting functions which might have an effect on system performance. This gives us the motivation to study new methods. In this paper, we investigate to design PSS with H_∞ control synthesis using linear matrix inequalities (LMI) constraint optimization technique. The LMI can effectively find the minimum H_∞ norm by convex optimization technique and be free from singular problems, whereas the solution of two algebraic Riccati equations is just a trial and error

* 正 會 員 : 湖南大 電氣工學科 助敎授・工博
** 正 會 員 : 忠南大 電氣工學科 博士修了
*** 正 會 員 : 忠南大 電氣工學科 敎授・工博
接受日字 : 1999年 7月 23日
最終完了 : 2000年 3月 14日

method to find optimal H_∞ norm and still needs to adjust weighting values of system matrices for non-singularity conditions. With the LMI method, it was also found that it is not necessary to know the exact and correct function of weighted filters but the roll-off and frequency band of the inverse of its magnitude in a certain frequency region are more important to attenuate external disturbances and noises. The detailed mathematical background, proofs and algorithms may be found in other publications shown in the References [10-12]. The H_∞ PSS depends on information available only at plant outputs such as terminal voltage and angular speed, thus, the design implementation is very simple and easy in the practical sense. Design results are simulated for a case study and check the system performance in comparison with currently operating lead/lag PSS and H_∞ PSS of standard two Riccati equations method.

2. Description of System Model

We briefly reviewed and derived the linearized power system model for low-frequency oscillation study in which a turbine-generator machine is connected to an infinite bus through double circuit transmission lines having a main step transformer and external impedance as shown in Fig. 1.

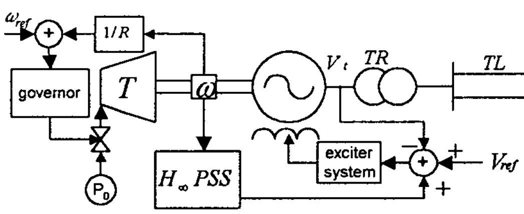

Fig. 1 System configuration of a turbine generator with infinite bus

Small signal stability problem will mostly happen in cases where a remote generation station sends a largeamount of power to a major power system through a relatively weak transmission line. This situation is adequately modeled by a single-machine infinite bus system. This model itself contains many uncertainties because not only is the network approximated as an infinite bus, which is assumed to be an external disturbance to the plant, but also a turbo-generator is simplified such that the fast dynamics are mostly neglected and time delayed dynamics are ignored.

The simplified generator model known as Park's two-axis machine model is used to describe the generator dynamics [13]. The excitation system is simply represented by the first order differential equation expressed in equation (5). The linear, time-invariant nominal design model, G_0, is obtained by linearizing around the nominal operating points shown in Fig. 2 and are expressed in the following equations;

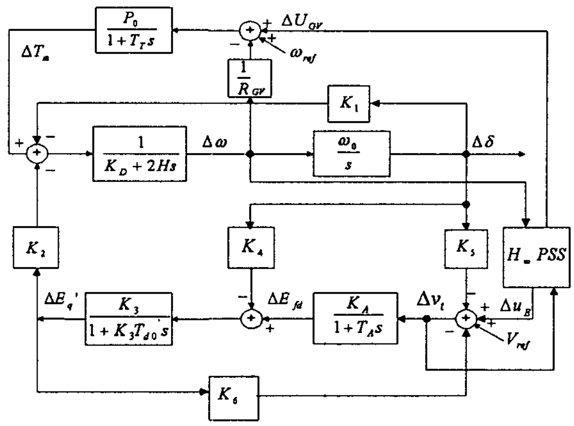

Fig. 2 Block diagram of linearized power system of Fig. 1

$$p\Delta T_m = \frac{1}{T_T}(P_0 \Delta U_{GV} - \frac{1}{R_{GV}}\Delta\omega_r - \Delta T_m) \quad (1)$$

$$p\Delta\omega_r = \frac{1}{2H}(\Delta T_m - K_D\Delta\omega_r - K_1\Delta\delta - K_2\Delta E_q') \quad (2)$$

$$p\Delta\delta = \omega_b \cdot \Delta\omega_r \quad (3)$$

$$p\Delta E_q' = \frac{1}{T_{d0}'}(\Delta E_{fd} - K_4\Delta\delta - \frac{1}{K_3}\Delta E_q') \quad (4)$$

$$p\Delta E_{fd} = \frac{1}{T_A}(K_A\Delta U_E - K_AK_5\Delta\delta - K_AK_6\Delta E_q' - \Delta E_{fd}) \quad (5)$$

$$P_{e0} = T_{e0} = \frac{E_{q0}'E_{B0}}{X_T}\sin\delta_0 \quad (6)$$

where $p = \frac{d}{dt}$, $K_1 = \frac{\partial T_e}{\partial\delta}\Big|_{E_q'=const}$, $K_2 = \frac{\partial T_e}{\partial E_q'}\Big|_{\delta=const}$,

$K_3 = \frac{X_d' + X_e}{X_d + X_e}$, $K_4 = \frac{1}{K_3}\frac{\partial E_q'}{\partial\delta}\Big|_{E_{fd}=const}$,

$K_5 = \frac{\partial E_t}{\partial\delta}\Big|_{E_q'=const}$, $K_6 = \frac{\partial E_t}{\partial E_q'}\Big|_{\delta=const}$

where all variables and constants for this study are expressed in per unit values and the symbols and main nomenclatures are defined in the Reference [13,14]. The linearized 5th order state variables and input variables are selected as ;

$$x(t) = [\Delta T_m(t), \Delta\omega(t), \Delta\delta(t), \Delta E_q'(t), \Delta E_{fd}(t)] \quad (7)$$

$$u(t) = [U_E(t), \Delta U_{GV}(t)] \quad (8)$$

3. System Perturbation and Robustness Requirements

3.1 System Perturbation Representation

Generally, system perturbation which is a source of system instability occurs mainly due to either system uncertainties or external disturbances. In this section, we discuss briefly the system uncertainties of two categories;

dynamical uncertainties and parameteric perturbations. Dynamical uncertainties appear dynamically to capture the effects of unmodeled dynamics such as neglecting the fast dynamics, invalid assumptions and model reduction. The problem for representing these uncertainties mathematically is that since the actual plant can never be known exactly, we cannot describe them mathematically in detail. Therefore, we adopt a set of membership for the uncertainties representation whose idea is to define a bounded set of system transfer function matrices. They are represented as the multiplicative uncertainties which have a relationship between actual plant $G(s)$ and nominal plant $G_0(s)$ given as norm bounded, frequency domain error with the following form ;

$$G(s)=\{G(s)\mid G(s)=[I+W(s)\Delta(s)]G_0(s),\ \|\Delta(jw)\|_\infty \le 1\} \quad (9)$$

where, $W(s)$ is the weighting function which encapsulates the system variation over a certain frequency range in which the uncertainty most likely occurs and $\Delta(s)$ is normalized to $\|\Delta(jw)\|_\infty \le 1$. And, $W(s)\Delta(s)=\delta_G(s)=\frac{G(s)-G_0(s)}{G_0(s)}$ is known as normalized multiplicative error with respect to the nominal plant model. Since the H_∞ norm of $\Delta(jw)$ is bounded by 1 and the phase and direction of $\Delta(jw)$ are allowed to vary arbitrarily, the uncertainties are contained in a bounded radius hypersphere $|W(j\omega)|$ at each frequency.

Therefore, $|W(j\omega)|$ may be seen as a frequency-dependent magnitude bound on these uncertainties as shown in Fig. 3. We can also consider the parametric perturbations whose dynamic behavior are defined by a set of operating parameters (for example ; $K_1,\cdots,K_6$) in the equations (1) to (5). In turn they are expressed as subject to change in the following equation (10) due to the parametric perturbations;

$$K_{0i}\,(1-\delta_{ki})<K_i<K_{0i}(1+\delta_{ki}) \ \text{ or } \ K_i=K_0(I+W_{ki}\Delta) \quad (10)$$

where K_{0i} is the nominal value of the system parameter and δ_{ki} is the upper bound of its variation. The class of this uncertainty may be described as $\delta_{ki}(s)=W_{ki}(s)\Delta(s)$with $\Delta(s)\in R\mid \|\Delta(jw)\|_\infty \le 1$. In Fig. 2 each of the individual parameters $K_1,\cdots,K_6$ should be replaced by its corresponding parametric uncertainties which tell us how the dynamics of the power system vary with different perturbations at various operating conditions and how the perturbed parameters behave in a way much closer to its real system. It is noted that the parametric uncertainties can not only address the multiple simultaneous perturbation but also preserve the structure information of uncertainties, which can also be represented as shown in Fig. 3[15].

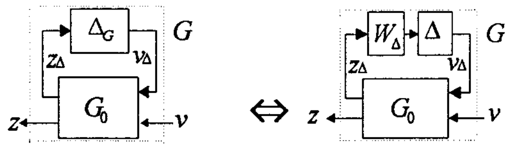

Fig. 3 Block diagram of generalized uncertainties

3.2 Closed Loop Performance and Robustness Requirements

3.2.1 Closed Loop System Description

The system uncertainties of Fig. 3 and external disturbances can be simply obtained by conducting the weighted function of input-output description as presented in the single closed loop interconnections to the generalized plant in Fig. 4. From Fig. 4, these can be described by the following matrix transfer function form of the multiple input and multiple output (MIMO) systems;

$$\begin{pmatrix} z_\Delta \\ z \end{pmatrix}=G\begin{pmatrix} v_\Delta \\ v \end{pmatrix}=\begin{pmatrix} G_{11} & G_{12} \\ G_{21} & G_{22} \end{pmatrix}\begin{pmatrix} v_\Delta \\ v \end{pmatrix}=\begin{pmatrix} M & G_{12} \\ G_{21} & G_{22} \end{pmatrix}\begin{pmatrix} v_\Delta \\ v \end{pmatrix} \quad (11)$$

where, $v_\Delta=\Delta\cdot z_\Delta$ and $M=\frac{z_\Delta}{v_\Delta}=-(I+KG)^{-1}K$ are the input-output function signals and closed loop transfer function as retrieved perturbation from the system uncertainties, respectively. v, z are the generalized external disturbances and controlled variables, and u, y are control inputs and measured outputs, respectively. All uncertainties may belong to a set Δ consisting of proper and stable transfer matrices. The controlled and uncontrolled interconnections are obtained as $u=K\cdot y$ and $v_\Delta=\Delta\cdot z_\Delta$ with $\|\Delta(jw)\|_\infty \le 1$ respectively. This leads to the linear frictional matrix transformation form[15];

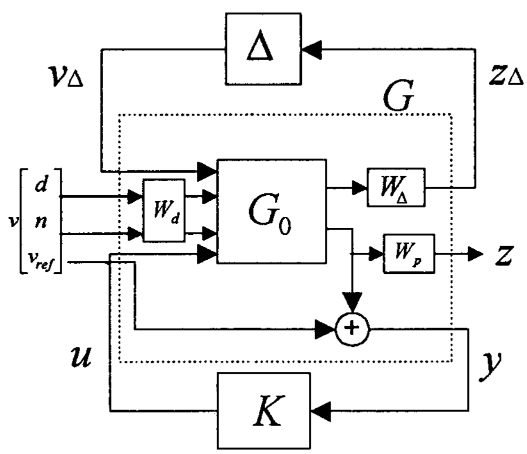

Fig. 4 Block diagram of generalized control system model

$$T_{zv}=(I+G_0K)^{-1}W_d \cdot W_p \quad (12)$$

$$T_{\Delta v\Delta z}=W_\Delta \cdot G_0K(I+G_0K)^{-1} \quad (13)$$

In order to setup the H_∞ control synthesis, the closed transfer function matrix (TFM) from the disturbance v to the desired output z is obtained by equation (12) in Fig. 4 (note that w_n, w_d are assumed W_v for convenience) and TFM from input z_Δ to v_Δ output as seen by Δ is also obtained by equation (13). It is noted that the system sensitivity TFM and complementary sensitivity TFM for the nominal feedback system are $S=(I+G_0K)^{-1}$and $C=G_0K(I+G_0K)^{-1}$, respectively.

3.2.2 Robustness Requirements Against System Uncertainties

By virtue of the small gain theorem[15,16], the internal stabilization condition under the presence of system uncertainties in equation (13) is given by the form of the H_∞ norm as the sufficient condition;

$$T_{\Delta v\Delta z}=\|W_\Delta G_0K(I+G_0K)^{-1}\|_\infty \le 1 \quad (14)$$

Using the definition of the H_∞ norm, an equivalent condition for stability robustness is expressed as;

$$\sigma_{\max}\{W_\Delta(jw)G_0(jw)K(jw)(I+G_0(jw)K(jw))^{-1}\}<1, \forall w \ge 0 \quad (15)$$

or $$\sigma_{\max}\{G_0(jw)K(jw)(I+G_0(jw)K(jw))^{-1}\}<\frac{1}{|W_\Delta(jw)|}, \forall w \ge 0 \quad (16)$$

Therefore, the system uncertainties may generally be described as norm bounded and frequency dependent uncertainties δ_G around the nominal plant G_0 in the form of $G(s)=G_0(I+\delta_G)$ In the sense that $\|W_\Delta\ \delta_G\|_\infty \le 1$, $\|W_\Delta(jw)^{-1}\|_\infty$ is considered as an upper bound of system uncertainties. And, if we select a scalar frequency-dependent weight as $\|W_\Delta(jw)^{-1}\|_\infty=w_\Delta(jw)^{-1}\cdot I=\gamma\cdot I$ and an H_∞ controller that achieves a specific value of γ, then, we can ensure that;

$$\sigma_{\max}[G_0(jw)K(jw)(I+G_0(jw)K(jw))^{-1}]<\gamma, \forall w \ge 0 \quad (17\ a)$$

$$a_{\max}[w_\Delta(jw)]<\frac{1}{\gamma}, \quad \forall w \ge 0 \quad (17\ b)$$

3.2.3 Robustness Requirements for External Disturbance Attenuations

The a priori information about external disturbances is always in the form of a certain frequency band in which their energy is concentrated. These kinds of disturbances can be expressed as a disturbance signal class of d which are weighted by a factor function $W_d(s)$ such that the H_2 norm of $\|W_d^{-1}\cdot d\|_2 \le 1$, which means that a certain frequency band in which the disturbances are mostly likely to be rejected. The disturbance attenuation can be described as minimum output for the worst case disturbance v in the above class. If we assume $W_p(s)=I$ in equation (12), this is also equivalent to minimizing the H_∞ norm of the weighted sensitivity function;

$$T_{zv}=\|(I+G_0K)^{-1}W_d\|_\infty \le 1 \quad \text{or} \quad (18)$$

$$\|S(jw)\|_\infty \le \frac{1}{|W_d(jw)|}, \quad \forall w \in \{0,\infty\} \quad (19)$$

Using the definition of the H_∞ norm, an equivalent condition for stability robustness is also expressed as;

$$\sigma_{\max}\{(I+G_0(jw)K(jw))^{-1}W_d\}<1, \quad \forall w \ge 0 \quad (20)$$

or

$$\sigma_{\max}\{(I+G_0(jw)K(jw))^{-1}\}<\frac{1}{|W_d(jw)|}, \quad \forall w \ge 0, \quad (21)$$

By the proper choice of scalar frequency-dependent weights, $W_d=w_d(s)I$ an H_∞ controller that achieves a specific value of γ ensures that;

$$\sigma_{\max}[(I+G_0(jw)K(jw))^{-1}]<\frac{\gamma}{|w_d(jw)|}, \quad \forall w \quad (22)$$

4. LMI Optimized H_∞ PSS Design

4.1 H_∞ Control Synthesis and Objective Function

The nominal feedback control system except uncertainties (Δ) and weighting filters (W_Δ, W_d, W_p) in Fig. 4 is applied to illustrate the fundamental concepts of H_∞ optimal control theory. The linear, time-invariant, continuous-time dynamical system for the worst case scenario may be considered with the following state-space representation ;

$$\begin{aligned}\dot{x}(t)&=Ax(t)+B_1v(t)+B_2u(t) \quad (23)\\ z(t)&=C_1x(t)+D_{11}v(t)+D_{12}u(t)\\ y(t)&=C_2x(t)+D_{21}v(t)+D_{22}u(t)\end{aligned}$$

where, $x\in R^{n\times 1}$, $v\in R^{m1\times 1}$, $u\in R^{m2\times 1}$, $z\in R^{p1\times 1}$, $y\in R^{p2\times 1}$ are state vector, exogenous inputs including disturbances and measurement noise, control input vector, regulated output, and measured output, respectively. $A\in R^{n\times n}$ is the system matrix, $B_1\in R^{n\times m1}$ is the exogenous input matrix, $C_1\in R^{p1\times n}$ is the control input matrix, $C_2\in R^{p2\times n}$ is the measured output matrix, $D_{11}\in R^{p1\times m1}$ is the regulated direct forward matrix,

$D_{12} \in R^{p1 \times m2}$ is the regulated direct forward matrix, $D_{21} \in R^{p2 \times m1}$ is the output direct forward matrix, and $D_{22} \in R^{p2 \times m2}$ is the output direct forward matrix. We wish to seek a linear, time-invariant, continuous controller of order n to reduce the effects of disturbances to the output and at the same time to enable the system to remain internally stable in the presence of system uncertainties of the form;

$$K \begin{cases} \dot{\hat{x}}(t) = A_k \hat{x}(t) + B_k y(t) \\ u(t) = C_k \hat{x}(t) + D_k y(t) \end{cases} \tag{24}$$

where $\hat{x}(t) \in R^n$ is the controller state vector. And it is equally expressed as the closed-loop transfer function matrix form;

$$U(s) = K(s) Y(s)$$
$$\text{where } K(s) = C_k (sI - A_k)^{-1} B_k + D_k \tag{25}$$

The basic idea of the H_∞ optimization problem is to minimize the $\|T(jw)\|_\infty$ which deals with the peak value of a certain closed-loop frequency response of a concerned system. In other words, we are to design a PSS controller to have the internal stabilizing and robust performance against the presence of both parametric perturbations and dynamic uncertainties and the worst case disturbances. The disturbances are considered to be an unknown but bounded L_2 signal. The object function of H_∞ optimization problem from equation (22) is expressed such that;

$$J = Min \|T_{zv}\|_\infty \tag{26}$$
$$\Rightarrow Find \sup_{w} \sigma_{\max}(T_{zv}(jw)) < \gamma$$

where $\|T_{zv}\|_\infty$ is the infinity(∞)-norm of the closed loop function from the exogenous input variable v to controlled variable z at a certain frequency, σ_{max} is the maximum singular value of this norm, and γ is the positive scalar value to determine as an index of boundness of the H_∞ norm. Where the energy gain(γ) of the closed loop system is analogously defined as the peak-to-peak gain in the following definition [15];

$$\gamma = \sup_{0 < \|v\|_2 < \infty} \frac{\|z\|_2}{\|v\|_2} = \sup_{w \in R} \sigma_{max}[T_{zv}(jw)] = \sup_{w \in R} \|T_{zv}(jw)\| \tag{27}$$

This means that the energy gain of stable linear time-invariant system is just equal to the H_∞ norm of the corresponding transfer matrix $\gamma = \|T_{zv}\|_\infty$ The closed loop transfer function T_{zv} including the central controller from the exogenous input v to the regulated output z is obtained as [15,16];

$$T_{zv}(s) = \frac{z(s)}{v(s)} = D_{cl} + C_{cl}(sI - A_{cl})^{-1} B_{cl} \quad n \tag{28}$$

$$\text{where } A_{cl} = \begin{pmatrix} A + B_2 D_k C_2 & B_2 C_k \\ B_k C_2 & A_k \end{pmatrix}, \quad B_{cl} = \begin{pmatrix} B_1 + B_2 D_k D_{21} \\ B_k D_{21} \end{pmatrix},$$

$$C_{cl} = (C_1 + D_{12} D_k C_2 \;\; D_{12} C_k) \qquad D_{cl} = D_{11} + D_{12} D_k D_{21}$$

4.2 Choice of Weighting Functions

From equation (17 b) the weighting function $W_d^{-1}(s)$ should be selected to be less than the H_∞ norm value (γ) of control objective function given by equation (26) for robustness performance against system uncertainties. Whereas $W_d(s)$ should be selected to attenuate all external disturbances (d, n) by maintaining a gain balance between the sensitivity function and the complementary sensitivity function. This means that the sensitivity function(S) may be made small at low frequency ranges for robustness against low frequency disturbances(d) and the complementary sensitivity function(C) may be made small at the high frequency ranges against high-frequency noises(n). Then, a trade-off is needed between $S(s)$ and $C(s)$, i.e., $S(s)$ is minimized at the low-frequency ranges while $C(s)$ is minimized at the high-frequency ranges since $C(s)$ and $S(s)$ cannot be simultaneously minimized due to $S(s)+C(s)=1$. A methodology for control system design consists of determining appropriate bounds on S and C, and adding a compensator to the plant to shape S and C in a such a way that they remain with the set bound, which is the so called "loop shaping" problem [16, 18].

Ideally, a comprehensive uncertainty and disturbance analysis should be made under all possible operating conditions to obtain precise information about system variation. However, the design problem for the worst case scenarios is that since the actual and perturbed plant can never be known exactly, the focus should be made to find the guaranteed smallest perturbation level that will de-stabilize the given system. In order to meet the above requirements by considering system frequency response in equation (22), the loop shaping specification is made by the followings.

- For external disturbances rejection, the gain of $S(s)$ should be minimized as much as possible at low frequency ranges.
- For sensor noises suppression, the roll-off of $C(s)$ gain should be approximated as $-40 dB/decade$ and

the gain should be less than $-20dB$ at $w=100rad/\sec$.

This specification is plotted as desirable frequency response shape in Fig. 5. The weighting functions(W_d, W_n) should be selected in such a way that they remain within the set bounds by adjusting H_∞ norm value (γ) to envelope the above specification curves of sensitivity and complementary sensitivity functions, respectively. As per the equation (22) they are found to be equation (29) which are shown Fig. 6 and 7 in this design ;

$$W_d^{-1}(s)=\gamma\cdot\begin{pmatrix}(s+0.01) & 0\\ 0 & (s+0.01)\end{pmatrix},$$

$$W_n^{-1}(s)=\begin{pmatrix}\frac{1000}{s^2} & 0\\ 0 & \frac{1000}{s^2}\end{pmatrix} \quad (29)$$

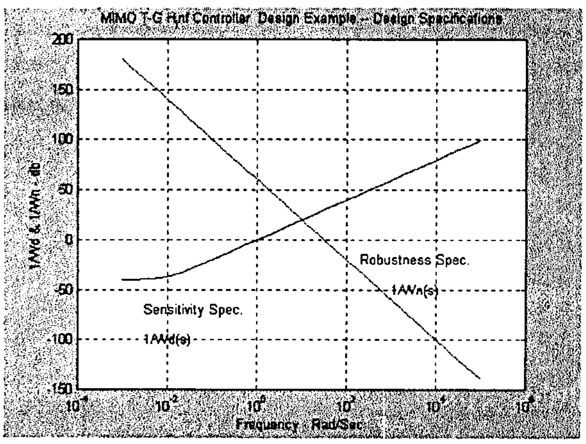

Fig. 5 Loop Shaping Specification of $W_d^{-1}(\omega)$ and $W_n^{-1}(\omega)$

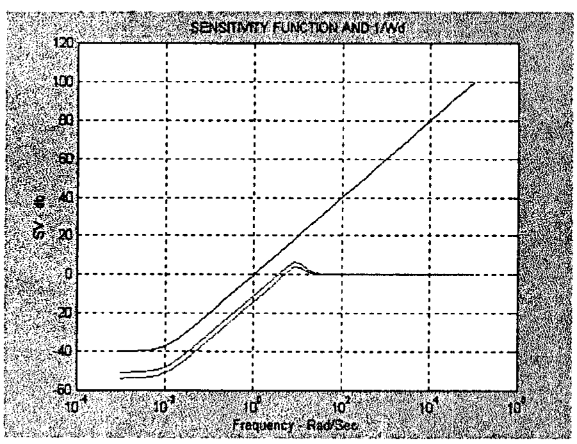

Fig. 6 Loop Shaping Plots; $W_d^{-1}(\omega)$ (upper curve) and $S(w)$ (lower ones) curves by adjusting $\gamma=1$ to $\gamma=3.2$

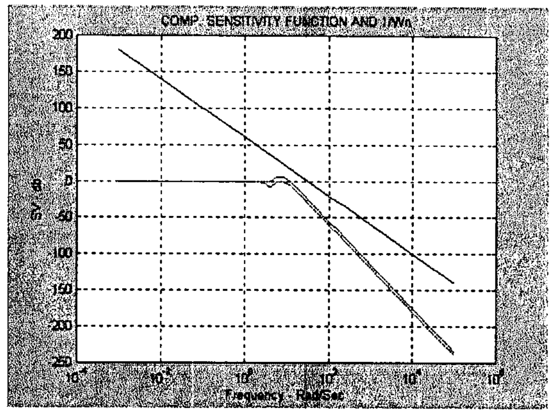

Fig. 7 Loop Shaping Plots; $W_n^{-1}(\omega)$ (upper curve) and $C(w)$ (lower ones) curves by adjusting $\gamma=1$ to $\gamma=3.2$

4.3 LMI H_∞-norm Optimization

The standard H_∞-norm optimization using the two Riccati equation solution method was originally developed by S. Doyle and K. Glover[4]. This is just a trial and error method to find the optimal γ such that two Riccati equations must be solved to avoid the singularity conditions of these equations. Furthermore, this still needs to consider weighting values to either satisfy design requirements or to satisfy the necessary feasibility conditions. Therefore, we approached to find the minimum H_∞ norm (γ) value using LMI convex optimization method. This LMI is efficiently computed and solved by the interior-point algorithm[12, 15].

By the virtue of the Bounded Real Lemma [11,15], A is stable (internal stability) and the H_∞ norm of T_{zv} is smaller than γ if and only if there exists a symmetric $X_{cl}>0$ with ;

$$\begin{pmatrix} A_{cl}^TX_{cl}+X_{cl}A_{cl} & X_{cl}B_{cl} & C_{cl}^T\\ B_{cl}^TX_{cl} & -\gamma I & D_{cl}^T\\ C_{cl} & D_{cl} & -\gamma I\end{pmatrix} < 0 \quad (30)$$

The unknown matrices are the LMI solution (X_{cl}) and controller matrices entering to A_{cl}, B_{cl}, C_{cl} and D_{cl}. Hence, this can be reduced to an LMI problem by elimination of controller matrices. With the notation of $\mho_k=\begin{pmatrix}A_k & B_k\\ C_k & D_k\end{pmatrix}$, the inequality (30) is written as;

$$Z+P^T\mho_kQ+Q^T\mho_k^TP < 0 \quad (31)$$

where the matrices Z, P and Q depend only on X_{cl} and the plant data. The elimination of the variable $\mho_k$ is addressed by the following Projection Lemma [10].

Lemma 4.1 (Projection Lemma [10])

Consider a symmetric matrix $Z \in R^{m \times m}$ and two matrices P and Q with column dimension m. Let W_P and W_Q denote any bases of the null space of P and Q, respectively. With this notation, there exists a matrix $\mho$ of compatible dimension such that $Z + P^T \mho Q + Q^T \mho^T P < 0$ if and only if $W_P^T Z W_P < 0$ and $W_Q^T Z W_Q < 0$.

By partitioning X_{cl} and X_{cl}^{-1} as;

$$X_{cl} = \begin{pmatrix} S & N \\ N^T & 0 \end{pmatrix}, \quad X_{cl}^{-1} = \begin{pmatrix} R & M \\ M^T & 0 \end{pmatrix} \tag{32}$$

where $R, S, M, N \in R^{n \times n}$. This lemma leads to the following LMI based solvability conditions for the sub-optimal H_∞ synthesis problem [10].

Theorem 4.2

Consider a proper continuous-time plant $G(s)$ of order n and realization system equations (9) and let N_{12} and N_{21} denote orthonormal bases of the null spaces of (B_2^T, D_{12}^T) and (C_2, D_{21}) respectively. The sub-optimal H_∞ problem of performance γ is solvable if and only if there exist two symmetric matrices $R, S \in R^{n \times n}$ satisfying the following system of LMIs [10] ;

$$\begin{pmatrix} N_{12} & 0 \\ 0 & I \end{pmatrix} \begin{pmatrix} AR + RA^T & RC_1^T & B_1 \\ C_1 R & -\gamma I & D_{11} \\ B_1^T & D_{11}^T & -\gamma I \end{pmatrix} \begin{pmatrix} N_{12} & 0 \\ 0 & I \end{pmatrix} < 0 \tag{33}$$

$$\begin{pmatrix} N_{21} & 0 \\ 0 & I \end{pmatrix} \begin{pmatrix} AS + SA^T & SB_1 & C_1^T \\ B_1^T S & -\gamma I & D_{11}^T \\ C_1 & D_{11} & -\gamma I \end{pmatrix} \begin{pmatrix} N_{21} & 0 \\ 0 & I \end{pmatrix} < 0 \tag{34}$$

$$\begin{pmatrix} R & I \\ I & S \end{pmatrix} > 0 \tag{35}$$

Then, LMI of equation (30) is converted to the following convex optimization problem.

$$J = Min\ f(x) < \gamma \tag{36}$$
$$\textit{subject to LMIs of (33), (34) and (35)}$$

The computing solution (γ, R, S) is a convex optimization problem and efficient algorithms are available to solve this feasibility problem in LMI toolbox[19] of MATLAB and SP code of the interior-point code. Any feasible pair (R, S) determines a set of full-order γ-suboptimal controllers as follows. First compute via SVD two invertible matrices $M, N \in R^{n \times n}$ such that

$$MN^T = I - RS \tag{37}$$

The bounded real lemma matrix X_{cl} is then uniquely determined by equation (32). Specially X_{cl} is the unique solution of linear equation as;

$$X_{cl} \begin{pmatrix} R & I \\ M^T & 0 \end{pmatrix} = \begin{pmatrix} 1 & S \\ 0 & N^T \end{pmatrix} \tag{38}$$

Once X_{cl} is determined, an adequate full-order controller is any solution $\mho_k$ of the controller LMI solved by the LMI toolbox in MATLAB. It can be summarized that the LMI-based H_∞ synthesis is performed in two steps[10].

① First solve a system of three LMIs where the unknowns are two symmetric matrices R and S of size equal to the plant order. These matrices determine an adequate closed loop Lyapunov function.

② Given γ, R, S and plant state space data, the controller matrix is computed by solving the controller equations.

5. Main Design and Simulation Results

5.1 Main Design Results of H_∞ PSS

An H_∞ optimization result is summarized in Table 1 by the interior-point algorithm computation which is available on LMI toolbox of MATLAB software package[19]. The design and initial operating conditions are summarized for a case study in Table 2 which assumes that a nominal system operates at conditions of active power $P_e = 0.9\ pu$, reactive power $Q_e = 0.3\ pu$, power factor $pf = 0.95\ (lag)$ and infinite bus voltage $E_B = 1.0\ pu$[14]. Singular values of the closed loop system with proposed H_∞ PSS are plotted in Fig. 8, which indicates that the maximum gain of design system is less than γ value at the frequency region of $10 rad/\text{sec}$ $(1.67 Hz)$ with the condition of bounded uncertainty level and attenuation of the weighted filters.

Table 3 shows the main design result in the form of state-space notation A_k, B_k, C_k and D_k with an optimal γ value. It is compared with the result of standard two Riccati equation method. We could get a smaller γ value which is more desirable for robustness requirements.

Table 1 Main Computation Results by LMI Optimization Method

Items	Computation Results
Optimal H_∞-Norm Performance	1.2188 (28 Iteration)
Best Objective Value in Feasible solution	1.218
Guaranteed Relative Accuracy	9.50e-003
Feasible Radius Saturation	2.449% of R = 1.00e+008

Table 2 Plant Parameter Data and Initial Operating Conditions [14]

System Parameters and Initial Values	System Matrix and Eigenvalues
Plant Parameter Data (P.U) $w_b = 2\pi f_b = 377$ $H = 3.82$, $K_D = 0.0026$, $R_{GV} = 0.05$, $T_T = 11.0\sec$ $R_a = 0.0037$, $X_d = 1.75$, $X_d' = 0.285$, $X_q = 1.68$, $X_q' = 0.47$, $R_e = 0.014$, $X_e = 0.4448$, $X_t = 0.1248$, $R_t = 0.0064$, $T_e = 0.95\sec$, $K_e = 200$, $V_{Max} = 3.5$, $V_{Min} = -3.5$ Initial P.U Values $P_0 = 1.0$, $\delta_0 = 80.5^\circ$, $P_{e0} = 0.9$, $Q_{e0} = 0.3$, $pf = 0.95$ (lag), $E_{B0} = 1.0\angle 0^\circ$, $T_{d0}' = 4\sec$ $E_{t0} = 1.026\angle 22.9^\circ$ $T_{q0}' = 0.54\sec$ $K_1 = 1.44778$, $K_2 = 1.31736$, $K_3 = 0.45312$, $K_4 = 1.2236$, $K_5 = -0.12$, $K_6 = 0.3$	A = [-0.0909 -1.818 0 0 0; 0.13089 -0.00034 -0.2082 -0.1963 0; 0 377 0 0 0; 0 0 -0.4505 0.7507 0.257; 0 0 28.2357 -70.5882 -1.1764] B_1^T = [0 0 1 0 ; 0 0 0 0 ; 0 0 0 0 ; 0 0 0 0 ; 0 0 0 0] B_2^T = [0.0909 0 0 0 0; 0 0 0 0 235.294]^T C_1 = [0 0 1 0 0 ; 0 0 0 0 0; 0 0 0 0 0] C_2 = [0 1 0 0 0; 0 0 -0.12 0.3 0] D_{11}^T = [0 0 0 0; 0 0 0 0; 0 0 0 0] D_{12}^T = [0 1 0; 0 0 1]^T D_{21} = [0 0 1 0; 0 0 0 1] D_{22} = [0 0; 0 0]
① State Variables : $x(t) = [\Delta T_m(t), \Delta w(t), \Delta\delta(t), \Delta E_q'(t), \Delta E_{fd}(t)]$ ② Control Variables : $u(t) = [U_E(t), \Delta U_{GV}(t)]$	
③ Exegous Inputs : $v(t) = [w_{ref}\ V_{ref}\ d\ n]$ $= [0\ 0\ T_B\ \theta]$	λ_i $= -0.4379 \pm 8.3308i$, $0.6505 \pm 5.1596i$, -0.0907

Table 3 Design Results Comparison between Standard Method and LMI Method

Item	Standard Two Riccati Equation Method	LMI Method
Optimal γ_{min} value	5.75 (No. of iteration : 12)	1.2188 (No. of iteration : 28)
eigenvalues (λ_i)	-2.2131±10.0710i, -3.4525±9.6664i, -0.907 -4.7937±4.6785i, -1.6310±3.9760i,	-4.0786±13.6170i, -1.5910±9.4261i, -0.922 -9.7005±5.7410i, -1.0948±4.7656i

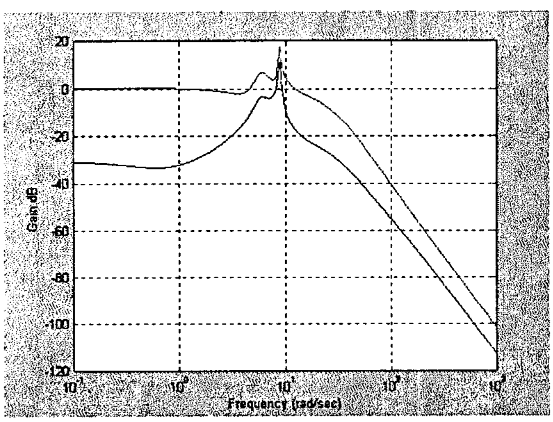

Fig. 8 Plot of singular values of the closed loop including designed PSS

5.2 Simulation and Performance Evaluation

The simulation conditions with state variables, control variables and control inputs are summarized in Table 1 as per proposed H_∞ PSS design consideration. Robustness performance against model uncertainties may be evaluated by the largest H_∞ norm of the uncertainties in order to guarantee the internal stability of closed system as per equations (14) and (17). In this design, the allowable bounded size of these uncertainties around frequence of $\omega_0 = 10\,rad/\sec$ ($1.67Hz$) are computed and evaluated as follows;

- Standard method : $\|\Delta\|_\infty = \frac{1}{5.75} = 0.174$

- LMI method : $\|\Delta\|_\infty = \frac{1}{1.218} = 0.8211$

This means that the maximum H_∞ norm of allowable uncertainties by standard and LMI methods are 0.174 and 0.8211, respectively. In addition, robustness performance against the worst case disturbance is evaluated by assigning external disturbances to the nominal plant with weighting filters. The worst case disturbance for simulation signal is assumed to be that the strong breaking torque (T_B) of equation (39) is suddenly loaded to the swing equation in equation (2) [13];

$$\frac{2H}{w_0}\frac{d^2\delta}{dt^2} = T_m - T_e - K_D\Delta w_r - T_B \qquad (39)$$

The magnitude of breaking torque is usually dependent on the location and type of event but the worst case disturbance in this simulation case used is a bounded L_2 signal of $T_B = 0.5\ p.u$ assuming 3-phase short circuit accident[13]. But, The zero mean and 2% covariance signals are also used as two sensor noises which have high frequency characteristics. In the case of nominal operating parameters $K_1, \ldots K_6$ Fig. 9 and Fig.10 show time responses of the deviation of rotating shaft angular speed and deviation of power angle and in the case of being changed operating parameters $K_1, \ldots K_6$ around 20% from nominal values, Fig. 11 and Fig. 12 show those respectively, where they are compared among LMI based H_∞ PSS(①), standard H_∞ PSS (②) and conventional lead/lag PSS(③). From these simulation results, the proposed H_∞ PSS design can provide the best damping effect for a synchronous generator over a wide range of operating conditions, and it provides guarantees to minimize the low-frequency oscillation of a closed-loop system and to maintain global system stability over the predetermined uncertainties and disturbances.

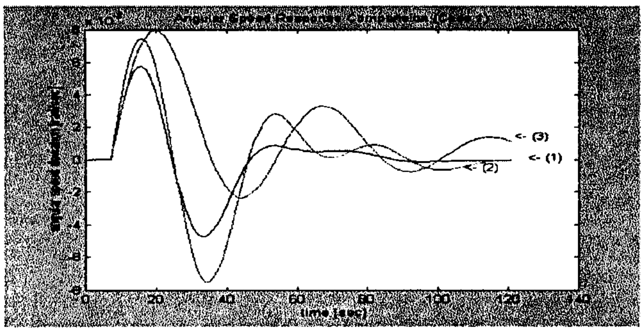

Fig. 9 Time Response of Angular Speed Deviation with Fixed Parameters (① LMI H_∞ ② Standard H_∞ ③ lead/lag PSS)

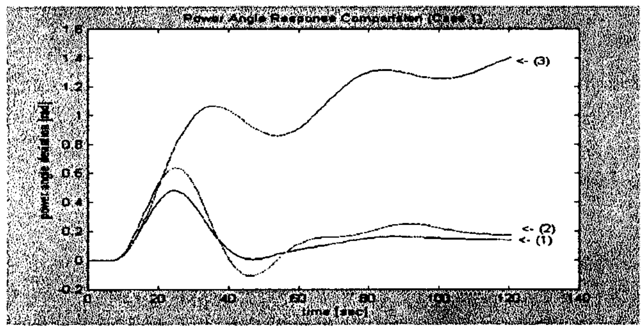

Fig. 10 Time Response of Power Angle Deviation with Fixed Parameters (① LMI H_∞ ② Standard H_∞ ③ lead/lag PSS)

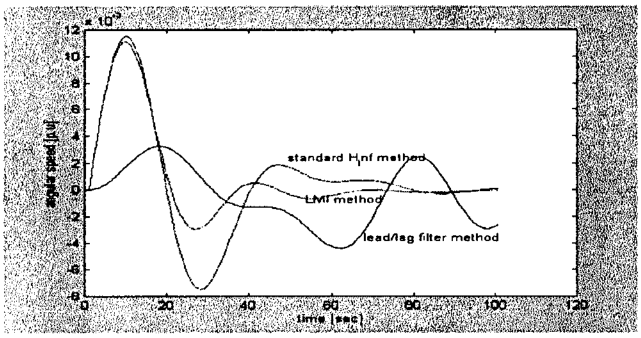

Fig. 11 Time Response of Angular Speed Deviation with Changed Parameters (① LMI H_∞ ② Standard H_∞ ③ lead/lag PSS)

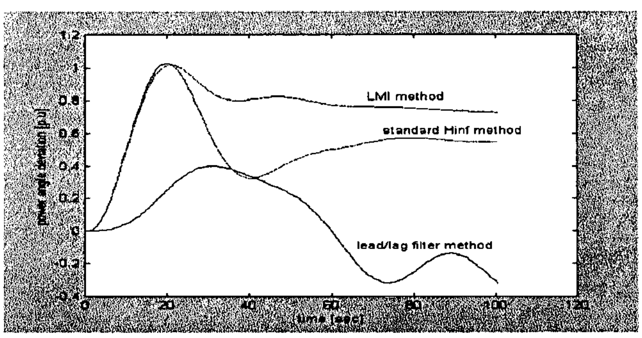

Fig. 12 Time Response of Power Angle Deviation with Changed Parameters (① LMI H_∞ ② Standard H_∞ ③ lead/lag PSS)

6. Conclusion

The design method of the H_∞-based PSS using LMI optimization technique has been designed to meet both the stability margins and disturbance attenuation requirements for robustness performance in terms of the H_∞ norm. The optimal H_∞ norm (γ) values of LMI method are compared with two Riccati solution methods and it is found that the LMI method is less level, which is more desirable for robust performance requirements. The proposed PSS is demonstrated by the performance comparison among standard H_∞ optimization PSS and conventional lead/lag PSS. Simulation results show that the proposed H_∞ PSS design can provide good damping effect for a synchronous generator over a wide range of operating conditions and the H_∞-based PSS design approach is superior in terms of the readily achievable closed-loop system performance under varying operating conditions. Therefore, we can conclude that proposed LMI based H_∞ PSS provides the guarantees to minimize the low-frequency oscillation and to maintain global system stability over the predetermined uncertainties and disturbances.

References

[1] A.A. Ghanakly and J.J. Dai, "Adaptive synchronous generator stabilizer design by generalized multi-variable pole shifting (GMPS) technique," IEEE Trans., PS-7(3) pp. 1239-1244, 1992.

[2] Q.H. Wu and B.W. Hogg, "Robust self-tuning regulator for a synchronous generator," IEE proc., Vol.135, pp 463-473, '88.

[3] D. Xia, "Self-tuning Controller for Generator excitation control", IEEE PAS, Vol. PAS-102,N0.6, 1877-1885, June, 1983.

[4] J.C. Doyle, K, Glover, "State-Space Solution to standard H_2 and H_∞ Control Problem", IEEE Autom. Control, vol. 38-N0. 8, pp 831-847, 1989. pp 53- 91, 1991.

[5] T.C. Yang, "Extending a stabilizer design method to multi-machine power systems", International Journal of Electrical Power and Energy Systems, vol. 17 (4), 1995

[6] T.C. Yang, "Applying H_∞ optimization method to power system stabilizer design", Electrical Power & Energy System, Vol. 19, No. 1, pp 29-35 & 37-43. 1997.

[7] S.S. Ahmed, L, Chen, A. Petroianu, " Robust H_∞ Tuning of Power System Stabilizers", IEEE/KTH Stockholm Power Tech Conference, Sweden, June 18-22, 1995.

[8] A.F. Komla, Y. Naoto, S. Hiroshi, " Synthesis of

two-input PSS based on the H_∞ Control Theory", Transaction of IEE Japan, Vol. 118-B, No. 6, 1998.
[9] S. Chen, O.P. Malik, " H_∞ optimization-based power system stabilizer design", IEE Proc.-Gener-Transm. Distrib., Vol. 142, No. 2, March, 1995.
[10] Pascal Gahinet, " Explicit Controller Formulas for Linear Matrix Inequality-based H_∞ Control Synthesis, Automatica, Vol, 32, No. 7, pp-1007-1014, 1996.
[11] S. Boyd and et al, "Linear Matrix Inequalities in System and Control Theory", SIAM, Applied Mathematics, 1994.
[12] Carsten Scherer and Siep Weiland, Lecture Notes DISC Course on Linear Matrix Inequalities in Control", version 2.0 , Delft University of Technology, April, 1999.
[13] Kundur, "Power System Stability and Control", McGraw-Hill, Inc, 1993.
[14] P.M, Anderson., A.A. Faud, "Power System Control and Stability", Iowa State University Press, 1977.
[15] Carsten Scherer, "Robust Control Theory", Delft University of Technology,1999.
[16] Bahram Shahian and Michael Hassul, "Control System Design using MATLAB", Prentice Hall, pp 421- 448, 1993.
[17] H. Kwakernaak, " Robust control and H_∞ optimization", Automatica, vol. 29, (13), pp 255-273, 1993.
[18] William S. Levine, "The Control Handbook Vol. I and II", CRC Press and IEEE Press, pp 595-606, 1996.
[19] Gahinet et al., 'LMI', 'Robust' and 'Control' MATLAB Tool-boxes for Control System Analysis and Design, Mathworks, Co.,

저 자 소 개

정 대 원 (鄭 大 源)

1957년 8월 6일 생. 1983년 부산 공대 전기공학과 졸업. 2000년 충남대 대학원 전기공학과 졸업(공박). 1982년~1990년 한국전력기술 선임기술원. 1990년~1997년 한국원자력연구소 선임연구원. 현재 호남대 공대 전기 공학과 조교수

Tel : 062-940-5494, Fax : 062-940-5077

E-mail : dwchung@honam.homan.ac.kr

주 운 표 (朱 雲 杓)

1956년 11월 3일생. 1984년 한양대 전기공학과 졸업. 1995년 충남대 전기공학과 박사과정수료 1988년~현재 한국원자력안전기술원 안전평가부 계측제어실 책임연구원

TEL : 042-868-0249, FAX : 042-861-2535

E-mail : zhu@kins.re.kr

김 건 중 (金 建 中)

1953년 2월 21일생. 1975년 서울대 공대 전기공학과 졸업. 1985년 동 대학원 전기공학과 졸업 (공박). 1977년 해군 제 2사관학교 교수. 현재 충남대 공대 전기공학과 교수

Tel : 042- 821-5659, FAX : 042-823-7970

E-mail : kjkim@ee.chungnam.ac.kr